

# OPTIMIZATION OF TENSILE STRENGTH AND PROCESSING TIME USING PCR-TOPSIS METHOD FOR FDM PROCESS

G.D. Lim<sup>1</sup>, M.J. Abd Latif<sup>2</sup>, M.R. Alkahari<sup>1</sup>, M.S. Yob<sup>1,2</sup>,  
S. Thapliyal<sup>3</sup> and L.R. Threemurthy<sup>4</sup>

<sup>1</sup>Faculty of Mechanical Engineering,  
Universiti Teknikal Malaysia Melaka, Hang Tuah Jaya,  
76100 Durian Tunggal, Melaka, Malaysia.

<sup>2</sup>Advanced Manufacturing Centre,  
Universiti Teknikal Malaysia Melaka, Hang Tuah Jaya,  
76100 Durian Tunggal, Melaka, Malaysia.

<sup>3</sup>National Institute of Technology,  
Warangal 506004, Telangana, India.

<sup>4</sup>PERKESO Rehabilitation Centre,  
Lot PT7263 Bandar Hijau, Hang Tuah Jaya,  
75450 Melaka, Malaysia.

Corresponding Author's Email: [juzaila@utem.edu.my](mailto:juzaila@utem.edu.my)

**Article History:** Received 6 August 2020; Revised 22 October 2020;  
Accepted 15 December 2020

**ABSTRACT:** Fused Deposition Modeling (FDM) is widely applied in industries due to its cost efficiency and capability to fabricate complex geometrical part. However, the main issues in FDM technology are the fabricated part strength and printing time. Therefore, this study aims to examine the FDM printing parameter to obtain the optimum tensile strength and printing time. Three most important parameters of layer thickness, nozzle diameter and printing velocity were studied to assess the tensile strength and processing time. Taguchi and PCR-TOPSIS methods were employed to evaluate the multi-response optimization problem. The tensile strength of FDM printed specimen was determined according to ASTM D638 while the processing time was computed from slicing software. From the results, the optimal parameter setting was achieved at 1.0mm nozzle diameter, 0.39mm layer thickness and 50mm/s printing velocity. In addition, printing velocity plays an important role toward the strength and printing time of FDM fabricated products followed by nozzle diameter and layer thickness.

**KEYWORDS:** *Fused Deposition Modeling; Additive Manufacturing; 3D Printing; Taguchi Method; PCR-TOPSIS*

## 1.0 INTRODUCTION

Fused Deposition Modeling (FDM) is one of the widely used 3D printing technique in additive manufacturing (AM) to fabricate prototype and functional parts since it was introduced in early 1990 [1]. The printing is perform using a heated extruder system to heat thermoplastic feedstock material in filament form up to a temperature above its melting point. The melted material is then extruded through a nozzle and deposited on a moving platform layer by layer from bottom to top in an orderly manner to construct 3D models as illustrated in Figure 1 [2].

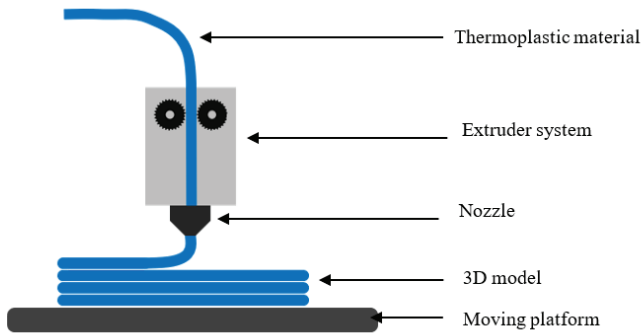


Figure 1: Schematic diagram of FDM technique

The FDM technique has significant advantages compare to other AM techniques including low maintenance cost, great simplicity, flexible material handling and wide variety of materials [2-3]. Although there are issues of poor surface roughness and inferior mechanical properties, the main drawback of FDM technique is low construction speed which relatively longer building time compare to other AM techniques such as selective laser sintering (SLS) and stereolithography (SLA) [1, 4] . Since, the reduction of product development cycle time is a major concern in industries, optimization of mechanical properties and construction speed is crucial to extend the application of FDM technology in industries [4-5].

The quality and printing time of FDM-produced product are greatly influenced by various process parameters such as printing velocity, layer thickness, raster orientation and infill percentage [6-7]. Although

extensive studies on analyzing and optimizing the FDM printing parameters have been carried out to obtain desirable outcome, most of the optimization studies were focused on improving single part's quality [8–10]. In this regard, Miazio [11] found that the increased of FDM printing velocity reduced the mechanical strength of the printed product. In other studies, the minimum processing time was achieved by increasing the layer thickness and feed rate to optimize the mechanical properties [7, 11]. The printing layer thickness is relatively related to the diameter of the printing nozzle which plays an important role in building time. It was reported that the nozzle diameter and layer thickness were the most significant factors on build time, tensile strength, and surface roughness of FDM printing products [12-13]. However, these important printing parameters are required to have thorough optimization analysis since most of the previous research examined each parameter in separate analysis.

In previous optimization studies, Taguchi method was widely used to determine optimal printing parameter. It is recognized as an efficient approach that improves the quality of the fabricated product [14-15]. However, the method is limited to single-response optimization and not suitable for optimizing multi-response problem. This is crucial because the 3D printing parameter optimization require more than one quality response [16]. The combination of Taguchi method, and Process Capability Ratio (PCR) and Technique for Order Performance by Similarity to Ideal Solution (TOPSIS) also known as PCR-TOPSIS were recognized as an efficient approach to perform the optimization of 3D printing parameter for multi-response problem [16-17].

Although the 3D printing parameters have been investigated, the studies were mainly focused to achieve either maximum mechanical strength or minimum printing time [9–11]. While adjusting the printing parameters could speed up the printing process, it also effected the strength of the printed component [18-19]. Therefore, this study aims to examine the FDM printing parameters to obtain the optimum tensile strength and printing time using PCR-TOPSIS optimization method.

## **2.0 METHODOLOGY**

In this study, three FDM printing parameters of nozzle diameter, layer thickness and printing velocity were considered to be the controlled printing parameters. Each parameter was tested at three different levels as shown in Table 1. Generally, most of the research were conducted using 0.4 mm nozzle diameter since it is the standard size installed in the commercial FDM 3D printers [18, 20]. The application of larger nozzle

diameter may allow for higher layer thickness and greatly reduce the total printing time. This study focused on the nozzle diameter above 0.4mm where the maximum layer thickness was set not to exceed 80% of the nozzle diameter and no restricted limit for the minimum layer height thickness [21]. The layer thickness was investigated from 0.3mm up to 0.48mm which was the maximum layer thickness for the 0.6mm nozzle diameter. Meanwhile, the printing velocity parameter was based on the recommendation from the material technical data between 30mm/s to 50mm/s. The Taguchi method was employed for the optimization study where the controlled parameters were arranged according to the Taguchi L9 orthogonal array as shown in Table 2. The tensile strength and processing time were evaluated for each experiment.

Table 1: FDM printing parameters testing levels

Printing parameter	Levels		
	1	2	3
Nozzle diameter (mm)	0.6	0.8	1.0
Layer thickness(mm)	0.3	0.39	0.48
Printing velocity (mm/s)	30	40	50

Table 2: Taguchi L9 orthogonal array

Experiment No.	Control Factors		
	Nozzle diameter	Layer thickness	Printing velocity
1	1	1	1
2	1	2	2
3	1	3	3
4	2	1	2
5	2	2	3
6	2	3	1
7	3	1	3
8	3	2	1
9	3	3	2

### 2.1 Specimen Preparation

The 3D model of the specimen was constructed using SolidWorks software according to ASTM D638 Type IV tensile specimen as shown in Figure 2. The model was saved as standard triangulation language (STL) format and then exported to IdeaMaker slicing software to convert into G-code file which was readable by the 3D printing machine. Three specimens ( $n=3$ ) were prepared for each experiment of printing combination parameters shown in Table 3. The specimens were printed using Raise3D Pro2 Plus 3D printing machine with polyamide (PA) material manufactured by Polymaker. All the specimens were printed at 100% infill percentage while the nozzle and heat bed temperatures were at 260°C and 70°C, respectively. The

printing time was obtained from the slicing software for further analysis. During the printing process, PA feedstock filament was kept in a heating chamber at 70°C to inhibit the material from absorbing moisture as PA is highly hydrophobic. Upon completion, the specimens were stored inside dry cabinet at 40% humidity and room temperature for at least 48 hours prior to the testing process.

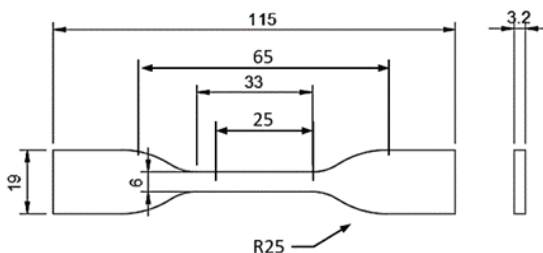


Figure 2: Dimension of testing specimen according to ASTM D638

Table 3: Combination of printing parameter for each experiment

Experiment No.	Control factors		
	Nozzle diameter (mm)	Layer thickness (mm)	Printing velocity (mm/s)
1	0.6	0.3	30
2	0.6	0.39	40
3	0.6	0.48	50
4	0.8	0.3	40
5	0.8	0.39	50
6	0.8	0.48	30
7	1.0	0.3	50
8	1.0	0.39	30
9	1.0	0.48	40

## 2.2 Tensile Test

The tensile tests were conducted according to ASTM D638 using Shimazu AGS-X Universal Testing Machine under the laboratory condition with temperature  $25 \pm 2^\circ\text{C}$  and relative humidity of  $55 \pm 10\%$ . The specimens were aligned at the axis of the center of the grip head and tighten firmly to prevent the slippage of the specimens during the test. The crosshead movement rate and the nominal strain rate at the start of the test are set at 5mm/min and 0.1mm/mm·min, respectively. The test was conducted until the specimen was loaded to failure and the value for tensile strength was recorded. The condition of the specimens before and after the tensile testing are shown in Figure 3.

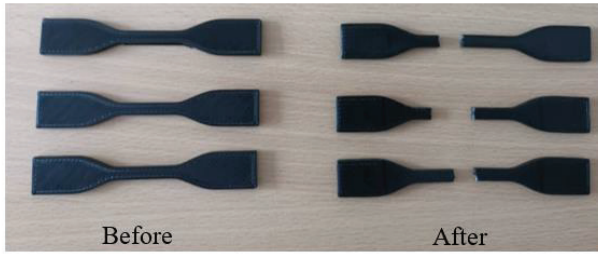


Figure 3: Specimens before and after the tensile test

### 2.3 Taguchi and PCR-TOPSIS Analysis

The Taguchi method was employed to compute the signal-to-noise ratio (SNR) of the tensile strength and printing time. SNR was utilized to describe the relative contributions of the true signal and the background noise. It is essential to measure the reliability of the received data and channel quality [22]. Based on the Taguchi method, two equations were applied to compute the SNR [23]. Equation (1) was used to obtain the response in a condition where smaller response produced better result. In contrary, Equation (2) was used to obtain the response when greater response contributed to a better result.

$$\eta_j^i = -10 \log_{10} \left[ \frac{1}{n} \sum_{i=1}^l y_j^i \right], 0 \leq y_j^i < \infty \quad (1)$$

$$\eta_j^i = -10 \log_{10} \left[ \frac{1}{n} \sum_{i=1}^l \frac{1}{y_j^i} \right], 0 \leq y_j^i < \infty \quad (2)$$

where  $y_j^i$  = observed data for the  $j$ th response at the  $i$ th trial.

$n$  = number of replications.

Following the SNR analysis, the optimum solution for multi-response of FDM printing parameter was determined using the PCR-TOPSIS method. The SNR was initially converted into dimensionless PCR to examine whether the printing parameters were capable to produce satisfying results [16]. Equation (3) shows the PCR of SNR in the  $j$ th response at the  $i$ th trial.

$$C_j^i = \frac{\eta_j^i - \bar{x}_{n_j}}{3s_{n_j}} \quad (3)$$

where  $\bar{x}_{n_j}$  is the sample mean for SNR in the  $j$ th response and  $s_{n_j}$  is the sample standard deviation for SNR in the  $j$ th response given as

$$\bar{x}_{n_j} = \frac{\sum_{i=1}^m \eta_j^i}{m-1} \quad (4)$$

$$s_{n_j} = \sqrt{\frac{\sum_{i=1}^m (\eta_j^i - \bar{x}_{n_j})^2}{m-1}} \quad (5)$$

Subsequently, TOPSIS was computed from the PCR of SNR to identify the relative closeness of each trial to the ideal solution. In TOPSIS, the preferred alternative was the one closest to the positive ideal solution and furthest away from the negative ideal solution [16]. Equation (6) demonstrates the preference value,  $S^i$  which gives the relative closeness of given alternative with ideal solution.

$$S^i = \frac{d^{i^-}}{d^{i^+} + d^{i^-}} \quad (6)$$

where  $d^{i^+}$  and  $d^{i^-}$  are the distance of  $i$ th trial from the positive and negative ideal solution respectively given as

$$d^{i^+} = \sqrt{\sum_{j=1}^n (C_j^i - C_j^+)^2}, \text{ for } i = 1, \dots, m \quad (7)$$

$$d^{i^-} = \sqrt{\sum_{j=1}^n (C_j^i - C_j^-)^2}, \text{ for } i = 1, \dots, m \quad (8)$$

provided that  $C_j^+ (C_j^-) = \max(\min)\{C_j^i, \text{ for } i = 1, 2, \dots, m\}$ .

### 3.0 RESULTS AND DISCUSSION

#### 3.1 Tensile Strength and Printing Time

The tensile strength and printing time for each experiment were tabulated in Table 4. Based on the results, the tensile strength was obtained ranging from 50.857 MPa to 65.786 MPa with 23% difference compared to maximum tensile strength. The maximum tensile strength was achieved in the Experiment 1 where the nozzle diameter was 0.6mm with the layer thickness set at 0.3mm and printing velocity of 30mm/s. It was also reported that higher tensile strength could be obtained using smaller nozzle diameter and thinner layer thickness [6, 24]. This is mainly due to the better adhesion between layers where smaller micro voids were produced between layers and created higher inter-layer bond. In addition, lower printing velocity provided better bonding time with the previous layer which will exhibit stronger fusion between layers and increased the tensile strength [11].

Table 4: Tensile strength and printing time of each experiment

Experiment No.	Tensile strength (MPa)					Printing time (minutes)
	1	2	3	Average	Standard deviation	
1	66.215	65.694	65.447	65.786	0.392	65.47
2	57.987	55.881	58.384	57.417	1.345	40.53
3	58.755	58.712	55.966	57.811	1.598	31.47
4	52.631	57.182	59.689	56.501	3.578	41.17
5	48.685	51.148	52.738	50.857	2.042	27.48
6	62.169	68.153	66.585	65.636	3.103	35.05
7	54.048	59.345	56.161	56.518	2.667	29.47
8	60.190	61.354	60.248	60.597	0.656	31.98
9	62.242	66.043	64.757	64.347	1.933	23.45

Meanwhile, the printing time was obtained from 23.45 minutes to 65.47 minutes with 179% difference compared to minimum printing time. The minimum printing time was observed in Experiment 9 due to its large nozzle diameter, high layer thickness and moderate printing velocity. Similar trend was also observed where the printing duration decreased when the printing nozzle diameter and layer thickness were increased [25]. This is due to the larger nozzle diameter allows for greater amount of material to be deposited per unit time, while higher layer thickness reduce the number of layers per unit length and reduced the total printing time [26-27]. Furthermore, the printing time was also found to be decreased when higher printing velocity was used as the nozzle traverses the printing area speed up [12].

### 3.2 PCR-TOPSIS Analysis

The SNR was computed for each experiment as a quality indicator for the printing parameter. The SNR analysis for the tensile strength response was conducted such that higher strength was always desirable. In contrary, the SNR analysis for the printing time response was based on shorter time was always preferable. Based on the SNR, the PCR-SNR values were calculated for each experiment as shown in Table 5. Based on results, the PCR-SNR values were within the specification tolerance of  $\pm 3$  standard deviation which indicates the satisfying quality of the printed specimens [28]. The optimum tensile strength and processing time were obtained in Experiment 1 due to the highest value of PCR-SNR.

Table 5: Result of SNR and PCR-SNR

Experiment No.	SNR		PCR-SNR	
	Tensile strength	Printing time	Tensile strength	Printing time
1	36.36	-36.32	0.28	-0.37
2	35.18	-32.16	0.25	-0.29
3	35.23	-29.96	0.26	-0.24
4	35.01	-32.29	0.25	-0.29
5	34.11	-28.78	0.23	-0.22
6	36.32	-30.89	0.28	-0.26
7	35.02	-29.45	0.25	-0.23
8	35.65	-30.10	0.26	-0.24
9	36.16	-27.40	0.27	-0.19

Further evaluation of printing parameter was performed using PCR-TOPSIS as shown in Table 6. From the results, Experiment 7 was nearly to the ideal combination with minimum  $d^{i+}$  value of 0.01 while Experiment 1 was the least ideal solution as the  $d^{i-}$  value was 0.38. The PCR-TOPSIS values were then used as a reference to determine the optimal condition of parameter setting.

Table 6: Result of PCR-TOPSIS

Experiment No.	$d^{i+}$	$d^{i-}$	PCR-TOPSIS
1	0.16	0.38	0.70
2	0.07	0.29	0.80
3	0.02	0.24	0.91
4	0.07	0.29	0.80
5	0.02	0.22	0.91
6	0.05	0.26	0.84
7	0.01	0.23	0.94
8	0.03	0.24	0.90
9	0.03	0.19	0.85

Subsequently, the mean value of PCR-TOPSIS for each parameter level was calculated and the main effect was plotted as shown in Table 7 and

Figure 4 respectively. The optimum condition was achieved at the combination of parameter levels with the highest average value. It was observed that the nozzle diameter, layer thickness, and printing velocity at Level 3 show the highest mean value compared to other levels. Similar finding was also reported in previous optimization study using statistical method where the optimized tensile strength and printing time were obtained when higher nozzle diameter and printing velocity were applied in the printing process [29]. However, the optimum layer thickness was at the intermediate value which was similar to the trend found in previous studies [30-31].

Table 7: Optimum condition

	Nozzle diameter	Layer thickness	Printing velocity
Level 1	0.804	0.814	0.814
Level 2	0.851	0.870	0.817
Level 3	0.896	0.867	0.920
Difference	0.092	0.054	0.107
Ranking	2	3	1
Optimum level	3	2	3

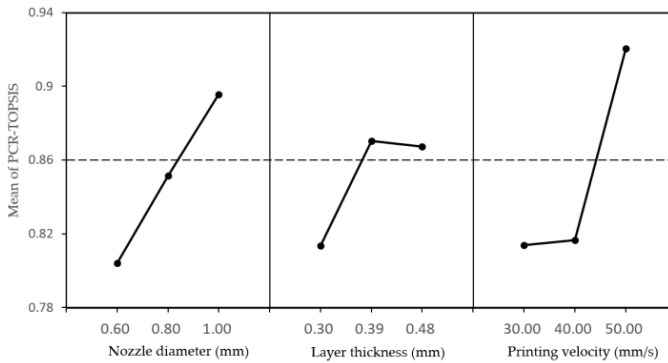


Figure 4: Main effect plot of PCR-TOPSIS

Based on these results, the optimum tensile strength and processing time of FDM printed component for PA material were obtained using 1.0mm nozzle diameter, 0.39mm layer thickness and 50mm/s printing velocity. The layer thickness was the least significant to a combination of optimized tensile strength and printing time with the PCR-TOPSIS value of 0.0537 while printing velocity was the most significant with 0.1065.

## 4.0 CONCLUSION

This study has successfully presented a systematic approach to determine the optimal 3D printing parameters by considering tensile strength and printing time using the combination of Taguchi and PCR-TOPSIS methods. The optimal nozzle diameter, layer thickness and printing velocity for FDM 3D printing of PA material was achieved to obtain the optimized tensile strength and printing time. Further study should be conducted with higher nozzle diameter and printing velocity. This could give an insight in producing high volume functional part and minimize the production cycle time.

## ACKNOWLEDGMENTS

This research is funded by Malaysian Technical University Network (MTUN) grant (Industri(MTUN)/PRPSB/2020/FKM-CARE/100047). The support from Universiti Teknikal Malaysia Melaka is gratefully acknowledged.

## REFERENCES

- [1] A. Dey and N. Yodo, "A systematic survey of FDM process parameter optimization and their influence on part characteristics," *Journal of Manufacturing and Materials Processing*, vol. 3, no. 64, pp. 1–30, 2019.
- [2] N. Shahrubudin, T. C. Lee, and R. Ramlan, "An overview on 3D printing technology: Technological, materials, and applications," *Procedia Manufacturing*, vol. 35, pp. 1286–1296, 2019.
- [3] C. E. Corcione, E. Palumbo, A. Masciullo, F. Montagna, and M. C. Torricelli, "Fused Deposition Modeling (FDM): An innovative technique aimed at reusing Lecce stone waste for industrial design and building applications," *Construction and Building Materials*, vol. 158, pp. 276–284, 2018.
- [4] A. D. Mazurchevici, D. Nedelcu, and R. Popa, "Additive manufacturing of composite materials by FDM technology: A review," *Indian Journal of Engineering and Materials Sciences*, vol. 27, no. 2, pp. 179–192, 2020.
- [5] S. K. Panda, S. Padhee, A. K. Sood, and S. S. Mahapatra, "Optimization of Fused Deposition Modelling (FDM) process parameters using bacterial foraging technique," *Intelligent Information Management*, vol. 1, no. 2, pp. 89–97, 2009.
- [6] M. Nabipour and B. Akhondi, "An experimental study of FDM parameters effects on tensile strength, density, and production time of ABS/Cu composites," *Journal of Elastomers and Plastics*, vol. 52, no. 3, pp. 1–19, 2020.

- [7] F. Rayegani and G. C. Onwubolu, "Fused deposition modelling (FDM) process parameter prediction and optimization using group method for data handling (GMDH) and differential evolution (DE)," *International Journal of Advanced Manufacturing Technology*, vol. 73, no. 4, pp. 509–519, 2014.
- [8] M. Á. Caminero, J. M. Chacón, E. García-Plaza, P. J. Núñez, J. M. Reverte, and J. P. Becar, "Additive manufacturing of PLA-based composites using fused filament fabrication: Effect of graphene nanoplatelet reinforcement on mechanical properties, dimensional accuracy and texture," *Polymers*, vol. 11, no. 5, pp. 1–22, 2019.
- [9] I. Durgun and R. Ertan, "Experimental investigation of FDM process for improvement of mechanical properties and production cost," *Rapid Prototyping Journal*, vol. 20, no. 3, pp. 228–235, 2014.
- [10] V. B. Nidagundi, R. Keshavamurthy, and C. P. S. Prakash, "Studies on parametric optimization for fused deposition modelling process," *Materials Today: Proceedings*, vol. 2, no. 4-5, pp. 1691–1699, 2015.
- [11] L. Miazio, "Impact of print speed on strength of samples printed in FDM technology," *Agricultural Engineering*, vol. 23, no. 2, pp. 33–38, 2019.
- [12] K. A. Al-Ghamdi, "Sustainable FDM additive manufacturing of ABS components with emphasis on energy minimized and time efficient lightweight construction," *International Journal of Lightweight Materials and Manufacture*, vol. 2, no. 4, pp. 338–345, 2019.
- [13] L. Yang, S. Li, Y. Li, M. Yang, and Q. Yuan, "Experimental investigations for optimizing the extrusion parameters on FDM PLA printed parts," *Journal of Materials Engineering and Performance*, vol. 28, no. 1, pp. 169–182, 2019.
- [14] S. Vyavahare, S. Kumar, and D. Panghal, "Experimental study of surface roughness, dimensional accuracy and time of fabrication of parts produced by fused deposition modelling," *Rapid Prototyping Journal*, vol. 26, no. 9, pp. 1535–1554, 2020.
- [15] Y. T. Yen, T. H. Fang, and Y. C. Lin, "Optimization of screen-printing parameters of SN9000 ink for pinholes using Taguchi method in chip on film packaging," *Robotics and Computer-Integrated Manufacturing*, vol. 27, no. 3, pp. 531–537, 2011.
- [16] H. C. Liao, "Using PCR-TOPSIS to optimise Taguchi's multi-response problem," *International Journal of Advanced Manufacturing Technology*, vol. 22, no. 10, pp. 649–655, 2003.
- [17] S. Athreya and Y. D. Venkatesh, "Application of Taguchi method for optimization of process parameters in improving the surface roughness of lathe facing operation," *International Refereed Journal of Engineering and Science*, vol. 1, no. 3, pp. 13–19, 2012.

- [18] J. Ten Kate, G. Smit, and P. Breedveld, "3D-printed upper limb prostheses: a review," *Disability and Rehabilitation: Assistive Technology*, vol. 12, no. 3, pp. 300–314, 2017.
- [19] M. Ouhsti, B. El Haddadi, and S. Belhouideg, "Effect of printing parameters on the mechanical properties of parts fabricated with open-source 3D printers in PLA by fused deposition modeling," *Mechanics and Mechanical Engineering*, vol. 22, no. 4, pp. 895–907, 2018.
- [20] S. P. Bhise, P. D. Pantanwane, and B. Rajiv, "Optimisation of hard turning of M42 tool steel using PCR-TOPSIS method," in *All India Manufacturing Technology, Design and Research Conference*, Guwahati, India, 2014, pp. 3–8.
- [21] V. E. Kuznetsov, A. N. Solonin, O. D. Urzhumtsev, R. Schilling, and A. G. Tavitov, "Strength of PLA components fabricated with fused deposition technology using a desktop 3D printer as a function of geometrical parameters of the process," *Polymers*, vol. 10, no. 3, pp. 1–11, 2018.
- [22] M. Bakkali, A. Stéphane, and S. Affes, "Generalized moment-based method for SNR estimation," in *IEEE Wireless Communications and Networking Conference*, Hong Kong, China, 2007, pp. 2228–2232.
- [23] R. Jeyapaul, P. Shahabudeen, and K. Krishnaiah, "Quality management research by considering multi-response problems in the Taguchi method - A review," *International Journal of Advanced Manufacturing Technology*, vol. 26, no. 12, pp. 1331–1337, 2005.
- [24] P. Shubham, C. Aggarwal, and S. Joshi, "Optimization of process parameter to improve dynamic mechanical properties of 3D printed ABS polymer using Taguchi method," *International Journal of Mechanical and Production Engineering*, vol. 6, no. 6, pp. 2321–2071, 2018.
- [25] W. Kiński and P. Pietkiewicz, "Influence of the printing nozzle diameter on tensile strength of produced 3D models in FDM technology," *Agricultural Engineering*, vol. 24, no. 3, pp. 31–38, 2020.
- [26] N. A. Sukindar, M. K. A. Ariffin, B. T. H. T. Baharudin, C. N. A. Jaafar, and M. I. S. Ismail, "Analyzing the effect of nozzle diameter in fused deposition modeling for extruding polylactic acid using open source 3D printing," *Jurnal Teknologi*, vol. 78, no. 10, pp. 7–15, 2016.
- [27] A. A. D'Amico, A. Debaie, and A. M. Peterson, "Effect of layer thickness on irreversible thermal expansion and interlayer strength in fused deposition modeling," *Rapid Prototyping Journal*, vol. 23, no. 5, pp. 943–953, 2017.
- [28] A. Rinanto, A. Nugroho, H. Prasetyo, and E. Pujiyanto, "Simultaneous optimization of tensile strength, energy consumption and processing time on FDM process using Taguchi and PCR-TOPSIS," in *International Conference on Science and Technology*, Bali, Indonesia, 2018, pp. 1–5.

- [29] K. K. Yang, J. H. Zhu, C. Wang, D. S. Jia, L. L. Song, and W. H. Zhang, "Experimental validation of 3D printed material behaviors and their influence on the structural topology design," *Computational Mechanics*, vol. 61, no. 5, pp. 581–598, 2018.
- [30] H. K. Dave, S. R. Rajpurohit, N. H. Patadiya, S. J Dave, K. S. Sharma, S. S. Thambad, V. P. Srinivasn, K. V. Sheth, "Compressive strength of PLA based scaffolds: Effect of layer height, infill density and print speed," *International Journal of Modern Manufacturing Technologies*, vol. 11, no. 1, pp. 21–27, 2019.
- [31] M. A. Kumar, M. S. Khan, and S. B. Mishra, "Effect of machine parameters on strength and hardness of FDM printed carbon fiber reinforced PETG thermoplastics," *Materials Today: Proceedings*, vol. 27, no. 2, pp. 975–983, 2020.